Biphasic adaptive evolution of antimicrobial resistance

Suman G. Das
Institute of Ecology and Evolution, University of Bern, Bern, Switzerland
Swiss Institute of Bioinformatics, Lausanne, Switzerland and
Institute for Biological Physics, University of Cologne, Cologne, Germany

Muhittin Mungan and Joachim Krug
Institute for Biological Physics, University of Cologne, Cologne, Germany
(Date: November 2, 2024)

A considerable body of work exists on the molecular biology of antimicrobial drug resistance, but general population dynamic principles of resistance evolution in microbial populations are still poorly understood. We study an empirically-motivated model of microbial evolution on drug-concentration dependent fitness landscapes. At any concentration a genotype's fitness depends on two phenotypes, the resistance level and the drug-free growth rate, with a tradeoff between these two. Adaptation on these landscapes at fixed drug concentration occurs in two phases. At first, the system evolves in a smooth region of the landscape with a rapid accumulation of resistance mutations accompanied by a decrease in the drug-free growth rate. In the second phase, there is partial recovery of the drug-free growth rate while the resistance level remains nearly constant. This recovery occurs on the rugged part of the landscape, is slow and involves the exchange of high-cost resistance mutations for low-cost ones. All changes occur via sequential origin-fixation events without any intermediate loss in fitness. We call this process *exchange compensation*, and note that it is distinct from the well-known phenomenon of fitness compensation that occurs through mutations at secondary sites when a resistant strain is re-cultured in a medium without drugs. The patterns of evolution in our two-dimensional phenotypic space of resistance and drug-less growth rate are independent of model details and therefore of wide relevance to understanding the tempo and mode of compensatory evolution.

The emergence of resistance to antimicrobial drugs is an urgent clinical problem. Prediction and control of drug resistance requires not only an understanding of the molecular mechanisms of resistance in microbes, but a quantitative grasp on the population dynamic aspects of resistance evolution as well [1–7]. A particular area of focus is how the structure of fitness landscapes (which capture the effect of gene-gene interactions, that is epistasis, on fitness) guide the evolution of antimicrobial resistance. A number of studies have constructed combinatorially complete landscapes comprising a small number of loci [4, 8–12], but our understanding of resistance evolution on large fitness landscapes and how it is impacted by the ambient drug concentration remains incomplete.

An important factor that affects the structure of landscapes is the tradeoff between resistance and null-fitness (*i.e.* the fitness in the absence of drugs). It has been reported in a large number of studies that resistance mutations often exhibit antagonistic pleiotropy on the two phenotypes of resistance and null-fitness, *i.e.* they increase the resistance while decreasing the fitness in the absence of drugs (see [13, 14] and references therein). A potential consequence of this is that bacteria selected for high resistance grow more slowly, thus affecting their transmission to new hosts and reducing their ability to cause widespread infection. However, experimental studies that culture resistant microbes in the absence of drugs find that they evolve to (partially) regain their null-fitness [1, 14–16]. The most commonly reported mode for this process is through compensatory mutations at secondary sites that do not compromise the acquired resistance [14, 16–18], though the contribution of the reversion of resistance mutations have been noted in some cases as well [15, 16, 19, 20].

Reduction of the cost of resistance can also happen in the presence of the drug [15, 21–24]. However, only a small number of empirical studies have directly addressed this question [17, 25, 26], despite its importance in determining the optimal course of drug treatment [15]. It has been found that the compensation loci and fitness effects in the presence of drugs can be different from those in its absence [17, 25], but due to the limited literature on the subject, there is no consensus on general mechanisms of compensatory evolution in the presence of drugs, or indeed on how generic it is.

In this paper, we study evolution on a theoretical fitness landscape with epistatic interactions where every resistance-increasing mutation also reduces the null-fitness. We observe that when the wild type is subjected to a fixed drug concentration, the initial evolutionary phase exhibits a gain in resistance accompanied by a loss in null-fitness, but a subsequent second phase shows a substantial amount of compensatory evolution even as the drug concentration stays constant. Moreover, compensation does not require mutations at secondary sites, but occurs through the reversal of high-cost resistance mutations and the substitution of low-cost ones. Contrary to common wisdom that regards compensatory mutations as a separate class of events, we show that they are an emergent feature of a model that contains only one class of mutations (namely, mutations

with antagonistic pleiotropic effects on resistance and null-fitness). It is the changing selection pressure along an evolutionary path that singles out mutations with qualitatively different phenotypic effects in the two phases of adaptation.

I. MODEL AND TERMINOLOGY

Fitness landscape model. We focus on an empirically-grounded model of tradeoff-induced landscapes (TIL model, see [27, 28]) to study the evolution of wild type bacteria exposed to a drug. For a given genotype $\boldsymbol{\sigma}$, the two relevant phenotypes are the resistance level $m_{\boldsymbol{\sigma}}$ quantified by the IC_{50} (the 50% inhibitory concentration), and the null-fitness (*i.e.,* the growth rate in the absence of drugs) denoted by $r_{\boldsymbol{\sigma}}$. Resistance comes at a cost, in the sense that resistance-increasing mutations reduce the null-fitness. The fitness of a genotype $\boldsymbol{\sigma}$ at drug-concentration x is represented by the bacterial growth rate, which is assumed to be given by a dose-response curve (DRC) of Hill type [29],

$$f_{\boldsymbol{\sigma}}(x) = \frac{r_{\boldsymbol{\sigma}}}{1 + (\frac{x}{m_{\boldsymbol{\sigma}}})^{\alpha}}, \tag{1}$$

where $\alpha > 0$ is the Hill coefficient.

The genotype is encoded by a binary vector $\boldsymbol{\sigma} = (\sigma_1, \ldots, \sigma_L)$, where L is the number of mutation sites of interest and $\sigma_i = 0, 1$ indicates the absence or presence of a mutation at locus i. We assume that the mutational effects on null-fitness and resistance are non-epistatic (multiplicative), that is

$$r_{\boldsymbol{\sigma}} = \prod_i {r_i}^{\sigma_i}, \qquad m_{\boldsymbol{\sigma}} = \prod_i {m_i}^{\sigma_i}. \tag{2}$$

This choice makes the model more analytically tractable, yet retains the features of adaptive evolution that we are interested in. Moreover, some experimental studies of antibiotic resistance evolution in bacteria show that Eq. (2) holds approximately [27, 30]. It is convenient to work with log-transformed parameters $u_i = -\ln r_i$, $v_i = \ln m_i$, $\chi = \ln x$, $F_{\boldsymbol{\sigma}} = \ln f_{\sigma}$. With this definition,

$$F_{\boldsymbol{\sigma}}(\chi) = -u_{\boldsymbol{\sigma}} - \ln(1 + e^{\alpha(\chi - v_{\boldsymbol{\sigma}})}) \tag{3}$$

where $u_{\boldsymbol{\sigma}} = \sum \sigma_i u_i$, $v_{\boldsymbol{\sigma}} = \sum \sigma_i v_i$ define the additive genotype-phenotype maps of u and v. The assumed tradeoff between resistance and null-fitness implies that $r_i < 1$, $m_i > 1$ and therefore $u_i > 0$, $v_i > 0$ for all i. Further, we impose the condition that

$$\frac{u_i}{v_i} < \alpha, \tag{4}$$

because, as shown later, any mutation violating this condition is always deleterious, and can thus be ignored.

The TIL model assumes universal antagonistic pleiotropy, in that every mutation affects both null-fitness and resistance in opposite directions. To generate large fitness landscapes, the $\{u_i\}$ and $\{v_i\}$ are taken to be random variables, where each pair (u_i, v_i) is drawn independently from a distribution $P(u_i, v_i)$ which respects the constraints imposed by the tradeoff and the condition Eq. (4). We denote $\bar{u} = \mathbb{E}[u_i]$ and $\bar{v} = \mathbb{E}[v_i]$, where $\mathbb{E}[\cdot]$ is the mean with respect to the joint distribution of u_i and v_i. Note that the TIL model has variable tradeoffs, that is, the value of the resistance benefit v_i does not uniquely determine the cost u_i.

Evolutionary dynamics. We are interested in the strong selection/weak mutation (SSWM) regime where selection is sufficiently strong so that only beneficial mutations can fix in the population, and mutations are sufficiently rare so that a new mutation occurs only after the previous mutation has been fixed or removed from the population [31]. In this limit, the evolutionary dynamics is an adaptive walk, in which the population moves along the fitness landscape in single mutational steps that each increase fitness. The walk terminates when the population reaches a local fitness peak, *i.e.* a genotype which has higher fitness than all other genotypes that are one mutation away. The probability that a *de novo* mutant $\boldsymbol{\sigma}'$ occurring in a population with genotype $\boldsymbol{\sigma}$ is fixed is given by the large population-size limit of the Kimura formula, $1 - e^{-2s}$ when the selection $s \equiv f_{\boldsymbol{\sigma}'}/f_{\boldsymbol{\sigma}} - 1 > 0$ and zero otherwise. We denote an adaptive walk with this fixation probability as the *Kimura adaptive walk*. We will also consider the *uniform adaptive walk*, where every fitter mutant has equal probability of being fixed [32]. A single time step of the adaptive walk consists of the origin and fate (fixation or extinction) of a mutation [33]. Therefore, the number of time steps is equal to the total number of mutations that have occurred (but not necessarily fixed).

II. RESULTS

We will first describe the broad features of the TIL fitness landscapes and the adaptive walks based on simulations. We then turn to a qualitative explanation of the adaptive evolution at a phenotypic level. Finally, we show that the results described in the first two subsections can be derived in precise mathematical terms, if we neglect the fluctuations in resistance by assuming that each mutation contributes a fixed amount v to the log-resistance $v_{\boldsymbol{\sigma}}$ of a genotype.

A. Directed and fluctuating phases of adaptation

The broad features of the fitness landscape and adaptive walks starting at the wild type are demonstrated schematically in Fig 1. Since both the null-fitness and the resistance contribute to the microbial fitness but there is a tradeoff between the two, fitness maxima are expected to have an intermediate number

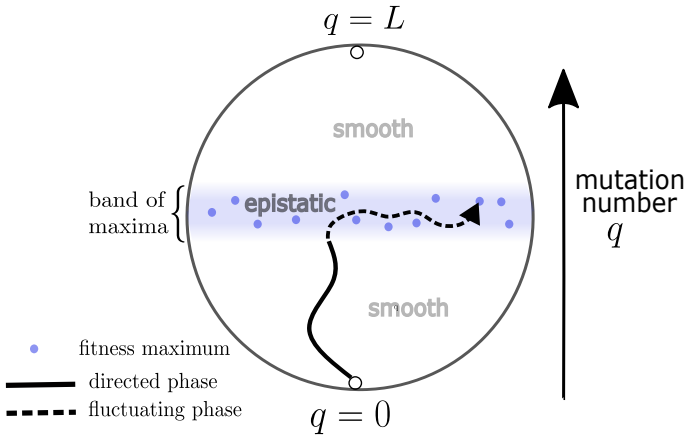

Fig 1. The figure depicts a schematic for visualizing the TIL model and adaptive walks on it. The genotypes are depicted as inhabiting the circle, and the number of mutations in the genotypes increases in the vertical direction. At any given concentration, the local fitness maxima (depicted as filled blue circles) contain a typical number of mutations, and therefore lie in a narrow band shaded in blue. An adaptive walk trajectory is shown as a black line. The walk begins at the wild type ($q = 0$) and terminates at one of the maxima. The trajectory has two phases. The solid part of the black line shows the directed phase, where the mutation number grows monotonically. The trajectory transitions to the fluctuating phase, marked with the dashed part of the black line, once the band of maxima is reached.

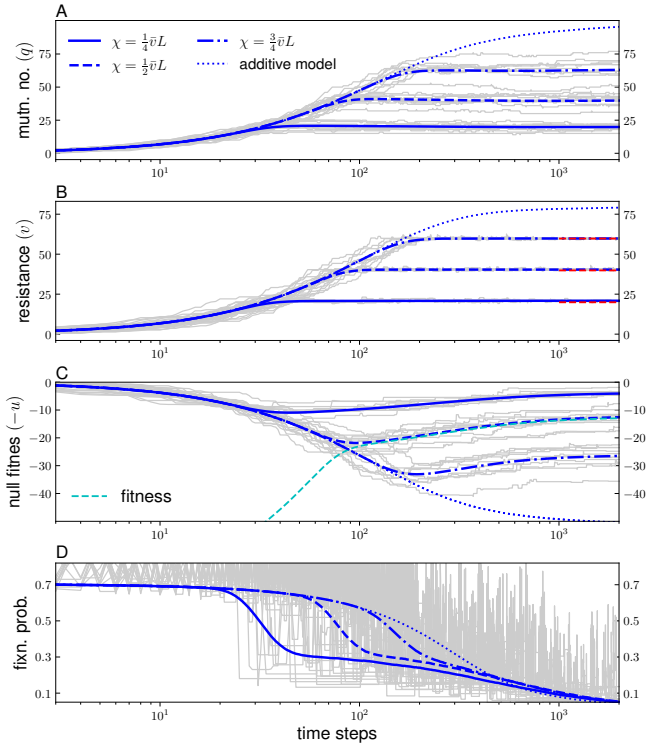

Fig 2. Numerical results for the mean of the various quantities associated with the evolving genotype are plotted. The mutational effect (u_i, v_i) is chosen from the distribution given in the Methods section, with $\mu = 0$. The genome size is $L = 100$. The colored lines are computed by generating a random landscape, simulating a Kimura adaptive walk, and averaging over 10^4 such realizations, while gray lines show individual trajectories. The dotted lines are averages for the additive model described by Eq. (5). (A) The mean mutation number and individual trajectories are shown for 3 different concentrations as indicated in the panel. The same concentrations are used in the remaining panels. (B) The mean resistance level saturates to a value close to χ (dashed red lines) in the fluctuating phase. (C) The null-fitness decreases in the directed phase and then grows in the fluctuating phase through the process of exchange compensation (see main text). The cyan line shows the fitness evolution for $\chi = \frac{1}{2}\bar{v}L$. The fitness closely follows the null-fitness as the resistance saturates to $v_{\boldsymbol{\sigma}} \simeq \chi$ in the fluctuating phase. (D) The fixation probability of all beneficial single-mutant genotypic neighbors of the evolving genotype are shown.

of mutations, the distribution of which is governed by χ. For large L and for $\chi \sim O(L)$, the leading order approximation to the mean number of mutations q^* in a fitness peak is given by $q^* \simeq \chi/\bar{v}$ (see [27] and SI text). The fitness peaks are located in a narrow band situated around q^* (Fig. 1).

An adaptive walk starting from the wild type has two distinct phases. The first is the *directed* phase, where the mutation number q in the evolving genotype increases monotonically (Fig. 2A). The term 'directed' refers to the fact that all fitness-increasing mutations in this phase are of the form $\sigma_i = 0 \to 1$, *i.e.* there is no reversal of acquired mutations and mutations accumulate. Naturally, this phase is associated with a monotonic increase in resistance along with a monotonic decrease in null-fitness, as shown in Fig. 2B and C. As depicted in Fig. 1, the directed phase ends once the walk enters the narrow band of maxima. The system now enters the *fluctuating* phase, where the mutation number can go down as well as the dynamics includes both forward ($0 \to 1$) and reverse ($1 \to 0$) mutations. In the fluctuating phase, the mean resistance is nearly constant whereas the mean null-fitness increases, leading to a partial recovery of the cost of resistance. Fig. 2C shows that the recovery is a slow process. This is partly due to the fact that there are fewer beneficial mutations, but also because there is a drop in the selection coefficients and therefore in the fixation probability of beneficial mutations, as seen in Fig. 2D. In fact, it is shown in SI Text and Fig. S2 that for large L the fixation probability undergoes a *sharp* transition between the two phases, in the sense that the time-scale over which the transition occurs is much smaller than the time-scale for the walk.

The origin of the directed phase can be understood as follows. Equation 3 together with Eq. (4) implies that when $\chi - v_{\boldsymbol{\sigma}} \gg \bar{v}$ (or equivalently $q^* - q_{\boldsymbol{\sigma}} \gg 1$), every forward mutation increases the fitness. In this phase, the fitness given by Eq. (3) can be approximated as $F \simeq$

$-u_{\boldsymbol{\sigma}} + \alpha v_{\boldsymbol{\sigma}} - \alpha\chi$. The constant term $\alpha\chi$ has no effect on the dynamics and can be dropped, leading to an additive version of the TIL model,

$$F_{\boldsymbol{\sigma}}^{\text{add}} = \sum_i \sigma_i(-u_i + \alpha v_i). \tag{5}$$

Thus, the system starting at the wild type ($q_{\boldsymbol{\sigma}} = 0$ and $v_{\boldsymbol{\sigma}} = 0$) traverses an effectively smooth landscape given by Eq. (5), acquiring mutations sequentially until its resistance reaches the value $v_{\boldsymbol{\sigma}} \simeq \chi$ (Fig. 2B). The departure of the full TIL model results from those of the additive model indicates the transition from the directed to the fluctuating phase, as seen in Fig 2.

The fluctuating phase exhibits compensatory evolution of the null-fitness. There are two notable features of this phase. Firstly, it demonstrates the role of epistasis in shaping evolutionary trajectories in this model. The fluctuating phase is a combination of forward and backward mutations, where the latter exhibits reversal of some of the resistance mutations acquired during the directed phase. Clearly, in the course of adaptive evolution, the effect of these mutations has switched from being beneficial (in the directed phase) to deleterious (in the fluctuating phase), exhibiting sign epistasis [34]. Although the genotype-phenotype map is additive, epistasis in fitness is introduced by the non-linear dependence of fitness F on the resistance v in Eq. (3), as noted in [27]. Secondly, we point out that compensatory evolution in this model occurs in the presence of universal antagonistic pleiotropy, in contrast to standard modes of compensatory evolution reported in the literature. Indeed, every reversal of a resistance mutation not only increases the null-fitness but also reduces the resistance. The role of pleiotropy in guiding the evolution of the phenotypes u and v is discussed in more detail in the next section.

B. Trajectories in phenotypic space and the role of pleiotropy

Several features of this model can be qualitatively understood purely at the phenotypic level by observing that (i) the DRC given by Eq. (3) furnishes a phenotype-fitness map, and (ii) evolution in the two-dimensional phenotypic space (u, v) is constrained by universal antagonistic pleiotropy, represented by the condition $u_i, v_i > 0$. A phenotypic mutation $(u, v) \to (u+u_i, v+v_i)$ induces a fitness change $\Delta F_i = \Delta F_i^u + \Delta F_i^v$, where

$$\Delta F_i^u = -u_i < 0,\ \Delta F_i^v = \log\left(\frac{1+e^{\alpha(\chi-v)}}{1+e^{\alpha(\chi-v-v_i)}}\right) > 0. \tag{6}$$

The quantity ΔF_i^v is monotonic increasing in χ and reaches the limit αv_i as $\chi \to \infty$. Thus, for a mutation with $u_i > \alpha v_i$, the fitness change ΔF_i is negative for all χ. Consequently, such a mutation will never be fixed, as noted before in Eq. (4). This also implies that the reversal of a mutation violating Eq. (4) is always beneficial, and it will eventually be lost if it happens to be initially present in the genotype.

The phenotype-fitness map implies that a mutant that is fitter than the wild type at concentration χ must satisfy the condition

$$u < u_{\max}(v) \equiv \log\left(\frac{1+e^{\alpha\chi}}{1+e^{\alpha(\chi-v)}}\right). \tag{7}$$

The function $u_{\max}(v)$ is the maximum cost that can be incurred in order to acquire resistance v, and further, $u < u_{\max}(v)$ delimits the region of the phenotypic space where adaptive evolution is possible. This is shown as the green shaded region in Fig 3A.

The role of pleiotropy is illustrated by the shape of the adaptive walk trajectories in the $u - v$ plane, plotted in Fig 3A (colored solid lines). In the directed phase, the trajectories become increasingly aligned with the direction of the maximum cost line (black curve) for systems with higher relative cost of resistance, characterized by $\bar{c} = \mathbb{E}[c_i]$, where $c_i = u_i/v_i$ is the *relative cost* of an individual mutation. In the fluctuating phase, there is a gain in mean null-fitness without loss of mean resistance, which may seem puzzling in the presence of antagonistic pleiotropy. The mechanism behind this becomes clearer upon examining specific sample trajectories (gray lines in Fig 3A). By looking closely at the individual adaptive steps (for example, those in the circle enclosing the fluctuating gray line in Fig 3A), we see that the null-fitness increases overall because the gain due to the reversal of resistance mutations is higher than the loss that occurs due to the forward mutations. Meanwhile, the resistance does not change substantially because the forward mutations occurring in the fluctuating phase counter the negative effect of the reversals on resistance. The model allows variable tradeoffs between u and v, implying that mutations conferring similar levels of resistance may differ considerably in their negative effects on null-fitness. The process proceeds by reversals that occur preferably on resistance mutations that have higher values of u_i and forward mutations that have lower values of u_i, without substantial alteration of v in the long run. This is treated in greater analytical detail in the next subsection through a special case of the TIL model where all mutations have the same v_i. We introduce the term *exchange compensation* to encapsulate the idea that in the fluctuating phase, compensation occurs by 'exchanging' acquired resistance mutations bearing a high cost for those with a low cost through a multi-step process. To put it succinctly, *the fluctuating phase selects against the strength of antagonistic pleiotropy while maintaining the resistance level.*

The effect of pleiotropy can be quantified through the evolution of the relative cost c_i associated with the substitutions. As noted before, c_i is bounded above by α (Eq. (4)), and bounded below by 0 (corresponding to a non-pleiotropic resistance mutation). Figure 3B

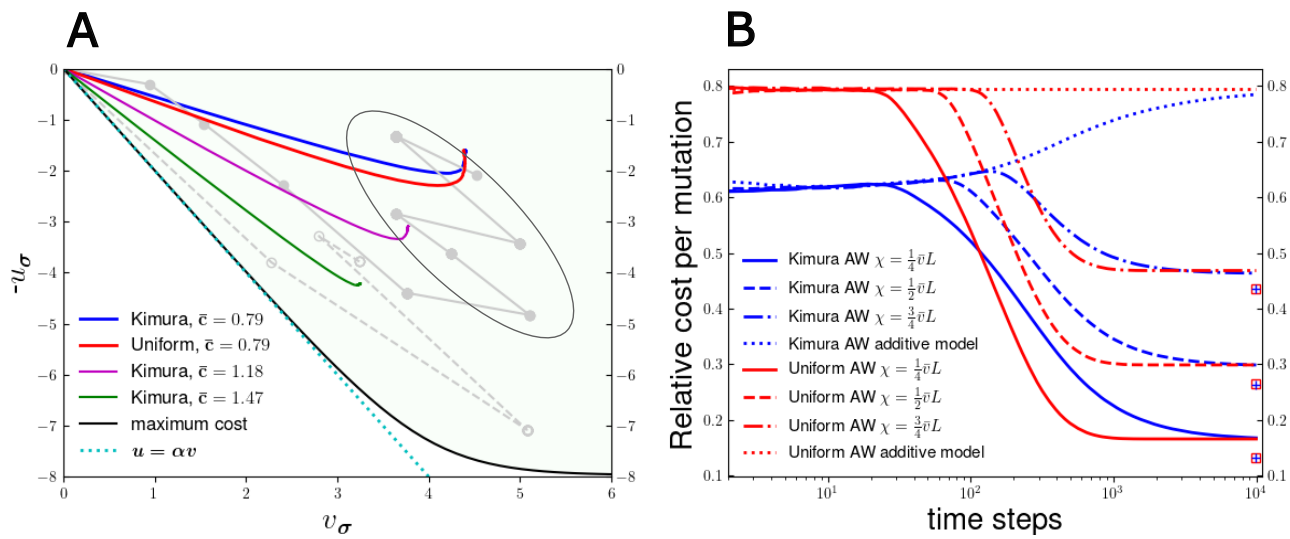

Fig 3. **A.**The plot shows the evolutionary paths in the $u - v$ plane for a genotype with $L = 10$ loci evolving at concentration $\chi = \frac{1}{2}\bar{v}L$. The colored solid lines are averages over 10^4 realizations. The constant $\bar{c}$ represents the mean relative cost of resistance mutations in the landscape. The distribution of the $\{u_i, v_i\}$ is given in Methods. The parameter μ is varied to tune $\bar{c}$ ($\mu = 0$ corresponds to $\bar{c} = 0.79$). The black line represents the upper bound of the net cost as given in Eq. (6). The green shaded region is the part of the phenotypic space to which adaptive walks are restricted. The curve $u = \alpha v$ (dotted cyan line) eventually deviates from the line of maximum cost since costly resistance mutations are no longer beneficial once a sufficiently high resistance level is achieved. Also shown are two individual trajectories at low cost (solid grey line) and high cost (dashed grey line). **B.** The plot shows the mean relative cost of the mutations present in the evolving genotype averaged over 10^4 realizations. The system size is $L = 100$ and all other parameters are the same as in Fig 2. Results are shown both for Kimura and uniform adaptive walks. The dotted lines represent the same quantity in the case of the additive model; the absence of compensation here is because lack of epistasis rules out reversals of mutations. The plus signs and squares represent the theoretical lower bounds averaged over 10^4 landscape realizations for the Kimura and uniform cases respectively.

summarizes the evolution of the mean relative cost of resistance mutations contained in the genotype, defined as $\left(\sum_i \sigma_i c_i\right) / \left(\sum_i \sigma_i\right)$, averaged over several landscape and walk realizations, and conditioned on at least one mutation being present in $\boldsymbol{\sigma}$. The results for the additive model in Eq. (5) are plotted as well. The points at which the additive model results diverge from the full TIL model indicate the end of the directed phase. As seen in the figure, the relative cost is high in the directed phase, and goes down as compensatory evolution occurs, reflecting the decreasing pleiotropic strength of the resistance mutations accumulating in the genotype. For the uniform adaptive walk, the mean relative cost in the directed phase (as given by the dotted red line) agrees with the expected relative cost of mutations in the full landscape, $\bar{c} \simeq 0.79$, since in the uniform walk all forward mutations are equally likely to be fixed in the directed phase

The Kimura walk behaves in a different way in the directed phase - there is a slight initial decrease since selection prefers both high v_i and low u_i, followed by a modest increase as low-cost resistance mutations become rarer. The maximum relative cost accrued by the Kimura walk (which occurs at the end of the directed phase) is lower than that of the uniform walk, which is expected since the former preferably fixes high-fitness mutants. The fluctuating phase of both the Kimura and uniform walks terminate with similar average values of the relative cost.

A lower bound on the per-mutation relative cost of a resistant genotype with n mutations is given by the mean of the n lowest c_i values from the pool of L mutations in the landscape. It is seen in Fig. 3B that the actual relative cost at the end of adaptive walks is not much higher than this bound, indicating that, within the constraints set by the number of resistance mutations, most of the cost is actually recovered through the process of compensation. Note that the degree of recovery for $L = 100$ in Fig. 3B is much higher than for the corresponding $L = 10$ case in Fig. 3A. Indeed, the degree of compensation increases with L, as shown in Fig S2, because for larger L the landscape contains mutations with values of u_i that extend closer to zero.

C. Mechanism of exchange compensation in a simplified setting

In the previous two subsections we have characterized the features of the biphasic adaptive evolution on TIL fitness landscapes. In order to understand better how this evolution emerges from the microsopic dynamics of single fitness increasing mutations, we now turn to a more detailed theoretical analysis.

As already shown, the adaptive evolution in the directed phase occurs on a smooth landscape that is well-approximated by the additive fitness function Eq. (5). The evolution proceeds through the sequential acquisition of forward mutations that increase resistance and reduce null-fitness. In other words, in this regime almost all fitness increasing transitions involve adding mutations. In the fluctuating phase, however, genotypes encounter a rugged region of the landscape, where both forward mutations (that increase fitness) and reverse mutations (that increase null-fitness) may be beneficial, depending on the genetic background in which they occur. In the following, we present a precise characterization of the topography of the fitness landscape in this regime and the adaptive evolution taking place on it. This will allow us to understand further the features described in the previous subsection, namely the emergence of compensatory mutation exchanges as well as the reduction of null-fitness at constant resistance.

For a given genotype $\boldsymbol{\sigma} = (\sigma_1, \ldots, \sigma_L)$, we define $I^+ = \{i : \sigma_i = 1\}$ as the set of loci at which there is a mutation. The complement I^- of this set specifies the loci where mutations are absent. In what follows we will alternatively specify a genotype $\boldsymbol{\sigma}$ in terms of its mutation set I^+ [27, 28]. For $i \in I^-$ we denote the genotype obtained from $\boldsymbol{\sigma}$ by adding a mutation at locus i as $\boldsymbol{\sigma}^{+i}$, likewise for $j \in I^+$, $\boldsymbol{\sigma}^{-j}$ is the genotype obtained from $\boldsymbol{\sigma}$ by reverting the mutation at locus j. For $i = 1, 2, \ldots, L$, we denote by χ_i the concentration at which the DRC's of the wild-type $\mathbf{0}$ and the single-mutant $\mathbf{0}^{+i}$ intersect and assume that the loci are indexed such that

$$\chi_1 < \chi_2 < \cdots < \chi_L. \tag{8}$$

Given a genotype with corresponding I^- non-empty and $i \in I^-$, the DRC's of $\boldsymbol{\sigma}$ and $\boldsymbol{\sigma}^{+i}$ will intersect at a concentration

$$\chi_{\boldsymbol{\sigma},+i} = \chi_i + \sum_{k \in I^+} v_k. \tag{9}$$

In particular, when $\chi > \chi_{\boldsymbol{\sigma},+i}$, the genotype $\boldsymbol{\sigma}^{+i}$ will have larger fitness than $\boldsymbol{\sigma}$, so that adding the mutation at i is fitness increasing. Note that given $\boldsymbol{\sigma}$, it is apparent from Eq. (9) that if χ is sufficiently large the addition of any mutation will be fitness increasing.

The genotype $\boldsymbol{\sigma}$ is a fitness peak at concentration χ, if for each $i \in I^-$ and $j \in I^+$, the genotypes $\boldsymbol{\sigma}^{+i}$ and $\boldsymbol{\sigma}^{-j}$ have lower fitness. From Eq. (9) it follows that this is equivalent to requiring that I^+ and $I^- = (I^+)^c$ are such that

$$\max_{i \in I^+} (\chi_i - v_i) < \chi - \sum_{k \in I^+} v_k < \min_{j \in I^-} \chi_j. \tag{10}$$

Details on extracting all fitness peaks from Eq. (10) are provided in [28].

Figure 2B indicates that in the fluctuating phase the statistical fluctuations in the resistance are far less than in the preceding directed phase. This suggests approximating the resistance $\sum_{k \in I^+} v_k$ of a genotype by its mean qv, where v is the average of v_i and $q = |I^+|$ is the mutation number. In this approximation, each mutation contributes an equal "quantum" v to the resistance of a genotype. We shall call this the q-TIL model. This approximation renders model analytically tractable, while retaining the key features of the adaptive evolution.

In the q-TIL model, the condition Eq. (10) for fitness peaks at χ becomes [1]

$$\max_{i \in I^+} (\chi_i - v) < \chi - qv < \min_{j \in I^-} \chi_j. \tag{11}$$

Letting

$$n = \left\lfloor \frac{\chi - \chi_1}{v} \right\rfloor, \qquad \text{and} \qquad \kappa = 1 + \left\lfloor \frac{\chi_L - \chi_1}{v} \right\rfloor, \tag{12}$$

where $\lfloor a \rfloor$ is the greatest integer less than or equal to a, and defining

$$K(\chi) = \max \{j : \chi_j < \chi\}, \tag{13}$$

one can deduce from Eq. (11) the following results

i. in terms of mutation number q, the fluctuating region is a strip of width κ, given by $n - \kappa + 1 \leq q \leq n + 1$, as shown in Fig. 4A,

ii. all fitness peaks at a given concentration χ have the same mutation number q^*, where q^* is the unique choice for q such that the following inequality holds:

$$K(\chi - qv) \leq q \leq K(\chi - qv + v). \tag{14}$$

The derivation of these results and further details on the topography of the fitness landscape of the q-TIL model will be presented elsewhere. The underlying key idea is the observation that given χ and q, the intersection points of Eq. (9) become $\chi_{\boldsymbol{\sigma},+i} = \chi_i + qv$ in the q-TIL model and in turn partition the set of loci into three subsets $\mathcal{L}_q = \{1, \ldots, k\}$, $\mathcal{M}_q = \{k+1, \ldots, k'\}$ and $\mathcal{R}_q = \{k'+1, \ldots, L\}$, where $k = K(\chi - qv)$ and $k' = K(\chi - qv + 1)$. For any locus $i \in \mathcal{L}_q$ ($j \in \mathcal{R}_q$) a transition is fitness increasing if and only if it involves adding (removing) a mutation at that locus, as illustrated in Fig.4B.

In the q-TIL model, the bi-phasic adaptation takes a particularly simple form when the width κ of the fluctuating region takes its smallest possible value $\kappa = 1$, so that the genotypes oscillate between $q = n$ and $q =$

[1] In the following we will be interested in genotypes that are neither the WT nor the all-mutant so that the sets $I^{\pm}$ satisfying the above inequalities are non-empty.

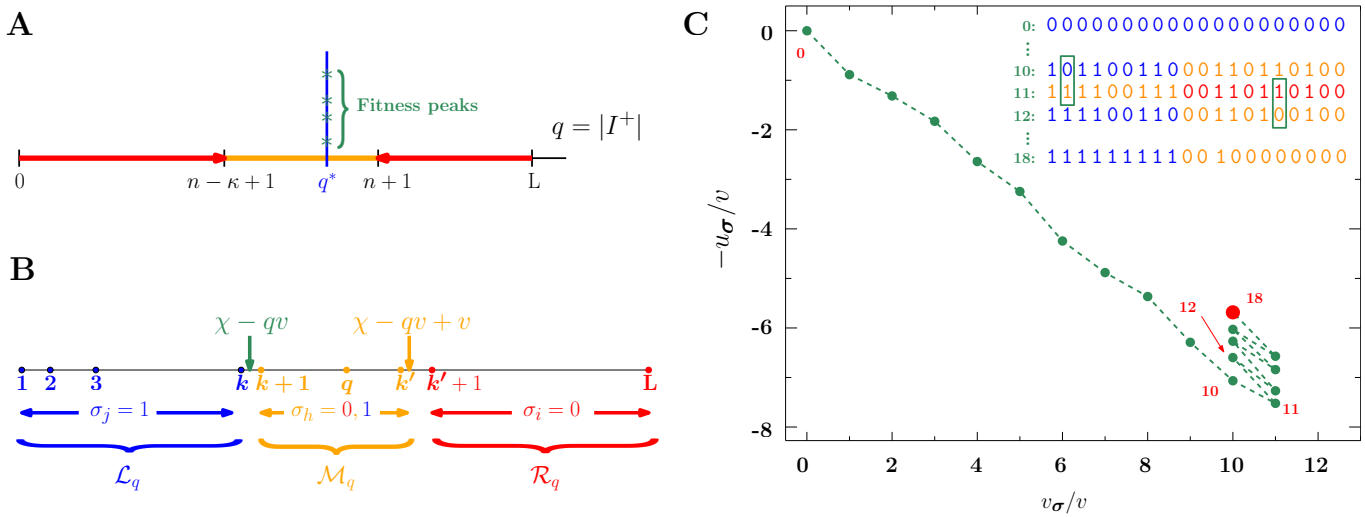

Fig 4. **The q-TIL model, a simplified version of the TIL model where each mutation confers the same resistance** v. A: All fitness peaks have the same mutation number q^* and the directed and fluctuating phases of evolution are determined by the range of mutation numbers indicated in red and orange respectively. In the directed phase (red) the arrows point in the direction of increasing fitness and thus move genotypes into the fluctuating regime (orange) which is trapping. B: The log-concentration χ together with the mutation number q of a genotype partition the set of loci into the three sets marked as $\mathcal{L}_q, \mathcal{M}_q$, and $\mathcal{R}_q$. For loci in $\mathcal{L}_q$ ($\mathcal{R}_q$) adding (removing) a mutation is always fitness increasing. C: Adaptive evolution in the $(u_{\boldsymbol{\sigma}}, v_{\boldsymbol{\sigma}})$ plane. Shown is a realization with $L = 20$ loci in the special case $\kappa = 1$. Step numbers are shown in red next to selected data points. Up to step 10, the adaptive walk is in the directed phase, where mutations pile up. In the fluctuating phase, the effective dynamics consists of *exchanging* mutation states of pairs of loci. The inset shows genotypic configurations at certain steps of the walk. Refer to text for further details.

$n+1$. This is illustrated in Fig.4C, showing the evolution of $u_{\boldsymbol{\sigma}}$ and $v_{\boldsymbol{\sigma}}$ for $L = 20$. The choice of concentration was such that $n = q^* = 10$ and $k = K(\chi - q^* v) = 9$.

Starting with the wild-type, the directed phase is characterized by mutation numbers $q \leq n$, cf. Fig.4A. In this regime, the set $\mathcal{L}_q$ is the set of all loci and therefore any mutation $0 \to 1$ increases fitness. As long as $q < n$, mutations are added one by one and as a result the log null-fitness $-u_{\boldsymbol{\sigma}}$ decreases monotonically, while the resistance $v_{\boldsymbol{\sigma}} = qv$ increases. Next, the walk enters the fluctuating phase at step 10, i.e. when $q = n = 10$, cf. Fig. 4C. The corresponding genotypic configuration is shown in the second row of the inset. The color coding of the mutation states of the individual loci follows that of the three regions depicted in Fig. 4B. Thus at step 10 the sites colored blue belong to $\mathcal{L}_q$, while those in orange constitute $\mathcal{M}_q$. Since $\kappa = 1$, the region $\mathcal{R}_q$ is empty. Therefore, the only available fitness increasing transitions at this step are $0 \to 1$ and must be selected from the loci colored blue.

At step 10 the locus $i = 2$ highlighted by the green box undergoes a mutation leading to the configuration at step 11. As a result, the mutation number increases by one, the pointers $\chi - qv$ and $\chi - qv + v$ decrease by v, and hence the assignment of the loci into the three regions changes (cf. inset of Fig. 4C). Now the only available fitness increasing transitions are from the $\mathcal{R}$-loci shown in red and they must remove a mutation. In the example shown, the site selected next is $j = 16$ and it is highlighted by the green box. The mutation number now decreases by one and we reach the genotype at step 12.

Observe that the net effect of going from step 10 to 12 has been the *exchange* of the mutation states of loci $i = 2$ and $j = 16$, while the mutation number remains the same. This is an example of exchange compensation. From Eq. (3) we see that, because the resistance $v_{\boldsymbol{\sigma}} = qv$ has not changed, the net change in log-fitness is equal to the change in null-fitness, $\Delta F_{\boldsymbol{\sigma}}(\chi) = -\Delta u_{\boldsymbol{\sigma}}$. Since we are considering adaptive walks, the change in log-fitness must be positive and therefore necessarily implies an increase of null-fitness. The increase of null-fitness in the fluctuating regime can be also verified directly via the mutation pathway by noting that, for the q-TIL model, the ordering Eq. (8) implies a corresponding ordering

$$u_1 < u_2 < \ldots < u_L. \tag{15}$$

Since the first and second mutation sites i and j are picked form $\mathcal{L}_{q^*}$ and $\mathcal{M}_{q^*}$, respectively, it is necessarily true that $j > i$. Hence, $-\Delta u_{\boldsymbol{\sigma}} = u_j - u_i$ is positive.

The adaptive walk in the fluctuating phase continues by the exchange of mutation states described above. As a result, the number of loci with mutation state 1 in $\mathcal{L}_{q^*}$ increases, terminating when all its k sites are mutated and leading to the fitness peak configuration shown in step 18 of Fig. 4C. Consequently, once a fitness peak has been reached, all sites $i = 1, 2, \ldots, k$ must be mutated, while the remaining sites carrying a mutation

are selected from the subset $\mathcal{M}_{q^*}$, cf. Fig. 4(B), and therefore characterize the individual fitness peaks. From Eq. (15) it is apparent that the sites $i = 1, 2, \ldots, k$ have the lowest null-fitness. Thus the null-fitness of a fitness peak reached has two contributions: a fixed part, $\sum_{1\leq i\leq k} u_i$, which is common to all fitness peaks, and a fluctuating part due to the selection of the remaining mutations from $\mathcal{M}_{q^*}$. The resulting null-fitness will therefore generally be larger than $\sum_{1\leq i\leq q^*} u_i$, consistent with the systematic deviation of asymptotic null-fitnesses from the lower bound in Fig. 3(B).

Finally, let us note that the case of general κ follows along similar lines. Once the fluctuating regime is entered, the mutation number q performs a random walk with reflecting boundaries at $q = n-\kappa+1$ and $q = n$, cf. Fig. 4A. Observing the genotype every time the mutation number becomes q^*, the change in log-fitness $\Delta F_{\boldsymbol{\sigma}}$ from one excursion to the next is simply $\Delta F_{\boldsymbol{\sigma}} = -\Delta u_{\boldsymbol{\sigma}}$ and hence the null-fitness continues to increase until a fitness peak is found and the walk terminates. Since the mutation number is q^* at the end of each excursion, the net effect on the genotype is a change of mutated loci.

III. DISCUSSION

In this work, we have identified two phases of adaptation to antimicrobial drugs that occur at constant drug concentration in a fitness landscape that incorporates universal tradeoffs between the mutational effects on resistance and null-fitness. The first phase involves resistance acquisition at the cost of null-fitness, and the second phase exhibits a partial recovery of the cost through a process we have called exchange compensation. Previous work has discussed the possibility of compensatory evolution occurring through a 'replacement' process, where high-cost mutants are replaced by equally resistant low-cost mutants, either by allelic replacement or mutations at different loci [17, 35]. Allelic replacement can occur through mutations that do not involve any intermediate low-resistance genotypes, but the nature of the hypothesized non-allelic replacement process has not been clarified. Exchange compensation is a specific mode of multi-step replacement that includes both reversions and fixation of new mutations. It involves individual mutational steps that can temporarily increase the cost or reduce the resistance, contrary to standard expectations from a compensatory process. Despite this, exchange compensation does not require crossing of any fitness valleys, because for every mutation that is fixed, the negative fitness effect of increased cost (or reduced resistance) is more than balanced by the increased resistance (or reduced cost) conferred by it. Rather than crossing fitness valleys, the adaptive evolution in the fluctuating regime proceeds along low dimensional ridges of the fitness landscape, the dimension of which is (in the case of the q-TIL model) bounded by the parameter κ.

A key element of our analysis is the nonlinear phenotype-fitness map (3). Previous work has employed phenotype-fitness maps to understand features of resistance and cost evolution. A theoretical treatment based on a two-dimensional trait space has shown how the assumption of two distinct phenotypic optima corresponding to absence and presence of drug can describe different scenarios of adaptation to drugs [24], and some of the resulting predictions have been confirmed experimentally [26, 36]. Our study goes beyond these abstract models by using phenotypic traits with a clear biological meaning that are mapped to fitness through the empirically validated DRC (1). Furthermore, our work illustrates how epistasis in the genotype-fitness map separates the dynamics into distinct phases.

We have used particular choices for the dose-response curve and the distribution of phenotypic effects to illustrate our results. However, the biphasic nature of evolution found here does not depend on these specific choices. The same qualitative features should be observed as long as two crucial requirements are satisfied. The first is that the dose-response curve should be such that when the resistance is sufficiently low, the dynamics should not involve reversal of resistance mutations even when they incur a high cost. This ensures the occurrence of the initial directed phase of evolution. It is shown in SI Text that this requirement is satisfied by a broad class of DRC's. The second requirement is that there should be variable tradeoffs, which is crucial to exchange compensation. This requirement is not a restrictive one either, since empirical studies across systems do not commonly find a strong relationship between individual mutational effects on resistance and their cost [14, 17, 37, 38]. Therefore, exchange compensation is not restricted to specific microbes or resistance mechanisms. Indeed, exchange compensation need not be limited to drug resistance evolution; it should occur whenever there are adaptational tradeoffs that satisfy the above-mentioned requirements.

Since exchange compensation is a slow process, its adverse effects will be most pronounced under long-term drug therapy. In line with the views of other authors [15, 39, 40], our work points to the need for better understanding of the optimal duration of a drug course. Of course, real-world scenarios can be more complicated due to other factors not considered in this theoretical study, such as the occurrence of compensatory mutations with no adverse effects on resistance, or high mutation supply which can help a population quickly traverse landscape minima that may be associated with the reversal of costly resistance mutations. However, the strength of our study is in demonstrating that reduction of the cost of resistance can happen in the long term even without these factors. Moreover, since the cost of resistance mutations drives their reversion in the absence of the drug [14], the reduction of the cost also reduces the likelihood for drug susceptibility

to be restored after treatment. While further work is needed to elucidate the role of additional factors that may complicate our modeling, the predicted generic nature of exchange compensation indicates the need for closer empirical and clinical scrutiny of the dynamics of compensatory evolution and the spread of resistance strains under long-term drug therapy.

IV. METHODS

Here we provide the details of the probability density and parameters used for the numerical results. For the phenotypic effects of mutations, we use the joint distribution

$$P(u_i, v_i) = \mathcal{N}^{-1} P_v(v_i) Q(u_i|v_i), \tag{16}$$

where

$$\begin{aligned} P_v(v_i) &= \exp\left(-\frac{v_i^2}{\sigma_v^2}\right) && \text{for } v_i > 0 \\ &= 0 && \text{otherwise,} \end{aligned} \tag{17}$$

and

$$\begin{aligned} Q(u_i|v_i) &= \exp\left(-\frac{(u_i-\mu)^2}{\sigma_u^2}\right)\Theta(\alpha v_i - u_i) && \text{for } u_i > 0 \\ &= 0 && \text{otherwise.} \end{aligned} \tag{18}$$

In the above, Θ is the Heaviside function and $\mathcal{N}$ is a normalization constant. In short, for each mutation, we choose v_i from a half-normal distribution, and then choose u_i from a truncated normal distribution where the factor $\Theta(\alpha v_i - u_i)$ ensures that the constraint Eq. (4) is obeyed. The parameter $\mu \geq 0$ controls the mean cost of the resistance mutations.

Throughout the paper, the simulations were done with parameter values $\alpha = 2$ and $\sigma_v = \sigma_u = 1$. Other parameter values are mentioned in the text and the figure captions as needed.

ACKNOWLEDGMENTS

This work was supported by Deutsche Forschungsgemeinschaft (DFG) within CRC 1310 “Predictability in Evolution”. MM was also supported by the DFG under Projektnummer 398962893.

[1] Bruce R Levin, Véronique Perrot, and Nina Walker. Compensatory mutations, antibiotic resistance and the population genetics of adaptive evolution in bacteria. *Genetics*, 154(3):985–997, 2000.

[2] Dan I Andersson and Diarmaid Hughes. Evolution of antibiotic resistance at non-lethal drug concentrations. *Drug resistance updates*, 15(3):162–172, 2012.

[3] Philip Greulich, Matthew Scott, Martin R Evans, and Rosalind J Allen. Growth-dependent bacterial susceptibility to ribosome-targeting antibiotics. *Molecular systems biology*, 11(3), 2015.

[4] C Brandon Ogbunugafor, C Scott Wylie, Ibrahim Diakite, Daniel M Weinreich, and Daniel L Hartl. Adaptive landscape by environment interactions dictate evolutionary dynamics in models of drug resistance. *PLoS computational biology*, 12(1):e1004710, 2016.

[5] Fernando Baquero, Jose L Martinez, V F. Lanza, Jerónimo Rodríguez-Beltrán, Juan Carlos Galán, Alvaro San Millán, Rafael Cantón, and Teresa M Coque. Evolutionary pathways and trajectories in antibiotic resistance. *Clinical Microbiology Reviews*, 34(4):e00050–19, 2021.

[6] Fernanda Pinheiro, Omar Warsi, Dan I Andersson, and Michael Lässig. Metabolic fitness landscapes predict the evolution of antibiotic resistance. *Nature Ecology & Evolution*, 5(5):677–687, 2021.

[7] Martijn F Schenk, Mark P Zwart, Sungmin Hwang, Philip Ruelens, Edouard Severing, Joachim Krug, and J Arjan GM de Visser. Population size mediates the contribution of high-rate and large-benefit mutations to parallel evolution. *Nature Ecology & Evolution*, 6(4):439–447, 2022.

[8] Daniel M. Weinreich, Nigel F. Delaney, Mark A. DePristo, and Daniel L. Hartl. Darwinian evolution can follow only very few mutational paths to fitter proteins. *Science*, 312:111–114, 2006.

[9] Martijn F Schenk, Ivan G Szendro, Merijn L M Salverda, Joachim Krug, and J Arjan G M de Visser. Patterns of epistasis between beneficial mutations in an antibiotic resistance gene. *Molecular biology and evolution*, 30(8):1779–1787, 2013.

[10] Portia M Mira, Juan C Meza, Anna Nandipati, and Miriam Barlow. Adaptive landscapes of resistance genes change as antibiotic concentrations change. *Molecular biology and evolution*, 32(10):2707–2715, 2015.

[11] Andrew D Farr, Diego Pesce, Suman G Das, Mark P Zwart, and J Arjan GM de Visser. The fitness of beta-lactamase mutants depends nonlinearly on resistance level at sublethal antibiotic concentrations. *MBio*, 14(3):e00098–23, 2023.

[12] Andrei Papkou, Lucia Garcia-Pastor, José Antonio Escudero, and Andreas Wagner. A rugged yet easily navigable fitness landscape. *Science*, 382(6673):eadh3860, 2023.

[13] Anita H Melnyk, Alex Wong, and Rees Kassen. The fitness costs of antibiotic resistance mutations. *Evolutionary applications*, 8(3):273–283, 2015.

[14] Dan I Andersson and Diarmaid Hughes. Antibiotic resistance and its cost: is it possible to reverse resistance? *Nature Reviews Microbiology*, 8(4):260, 2010.

[15] Paulo Durão, Roberto Balbontín, and Isabel Gordo. Evolutionary mechanisms shaping the maintenance of

antibiotic resistance. *Trends in microbiology*, 26(8):677–691, 2018.

[16] Sophie Maisnier-Patin and Dan I Andersson. Adaptation to the deleterious effects of antimicrobial drug resistance mutations by compensatory evolution. *Research in microbiology*, 155(5):360–369, 2004.

[17] Mary G Reynolds. Compensatory evolution in rifampin-resistant escherichia coli. *Genetics*, 156(4):1471–1481, 2000.

[18] Amel Kevin Alame Emane, Xujun Guo, Howard E Takiff, and Shengyuan Liu. Drug resistance, fitness and compensatory mutations in mycobacterium tuberculosis. *Tuberculosis*, 129:102091, 2021.

[19] J Bjorkman, I Nagaev, OG Berg, Diarmaid Hughes, and Dan I Andersson. Effects of environment on compensatory mutations to ameliorate costs of antibiotic resistance. *Science*, 287(5457):1479–1482, 2000.

[20] Ivan Nagaev, Johanna Björkman, Dan I Andersson, and Diarmaid Hughes. Biological cost and compensatory evolution in fusidic acid-resistant staphylococcus aureus. *Molecular microbiology*, 40(2):433–439, 2001.

[21] Andreas Handel, Roland R Regoes, and Rustom Antia. The role of compensatory mutations in the emergence of drug resistance. *PLoS computational biology*, 2(10):e137, 2006.

[22] Pia Schulz zur Wiesch, Jan Engelstadter, and Sebastian Bonhoeffer. Compensation of fitness costs and reversibility of antibiotic resistance mutations. *Antimicrobial agents and chemotherapy*, 54(5):2085–2095, 2010.

[23] Michael Baym, Tami D Lieberman, Eric D Kelsic, Remy Chait, Rotem Gross, Idan Yelin, and Roy Kishony. Spatiotemporal microbial evolution on antibiotic landscapes. *Science*, 353(6304):1147–1151, 2016.

[24] T Lenormand, N Harmand, and R Gallet. Cost of resistance: an unreasonably expensive concept. *Rethinking Ecology*, 3:51–70, 2018.

[25] Wilhelm Paulander, Sophie Maisnier-Patin, and Dan I Andersson. Multiple mechanisms to ameliorate the fitness burden of mupirocin resistance in salmonella typhimurium. *Molecular microbiology*, 64(4):1038–1048, 2007.

[26] Noémie Harmand, Romain Gallet, Guillaume Martin, and Thomas Lenormand. Evolution of bacteria specialization along an antibiotic dose gradient. *Evolution Letters*, 2(3):221–232, 2018.

[27] Suman G Das, Susana OL Direito, Bartlomiej Waclaw, Rosalind J Allen, and Joachim Krug. Predictable properties of fitness landscapes induced by adaptational tradeoffs. *Elife*, 9:e55155, 2020.

[28] Suman G Das, Joachim Krug, and Muhittin Mungan. Driven disordered systems approach to biological evolution in changing environments. *Physical Review X*, 12(3):031040, 2022.

[29] Roland R Regoes, Camilla Wiuff, Renata M Zappala, Kim N Garner, Fernando Baquero, and Bruce R Levin. Pharmacodynamic functions: a multiparameter approach to the design of antibiotic treatment regimens. *Antimicrobial agents and chemotherapy*, 48(10):3670–3676, 2004.

[30] Michael Knopp and Dan I Andersson. Predictable phenotypes of antibiotic resistance mutations. *mBio*, 9(3):e00770–18, 2018.

[31] John H. Gillespie. Molecular evolution over the mutational landscape. *Evolution*, 38:1116–1129, 1984.

[32] Stuart Kauffman and Simon Levin. Towards a general theory of adaptive walks on rugged landscapes. *Journal of theoretical Biology*, 128(1):11–45, 1987.

[33] David M McCandlish and Arlin Stoltzfus. Modeling evolution using the probability of fixation: history and implications. *The Quarterly review of biology*, 89(3):225–252, 2014.

[34] Daniel M Weinreich, Richard A Watson, and Lin Chao. Perspective: Sign epistasis and genetic costraint on evolutionary trajectories. *Evolution*, 59(6):1165–1174, 2005.

[35] Frederick M Cohan, Elaine C King, and Piotr Zawadzki. Amelioration of the deleterious pleiotropic effects of an adaptive mutation in bacillus subtilis. *Evolution*, 48(1):81–95, 1994.

[36] Noémie Harmand, Romain Gallet, Roula Jabbour-Zahab, Guillaume Martin, and Thomas Lenormand. Fisher's geometrical model and the mutational patterns of antibiotic resistance across dose gradients. *Evolution*, 71(1):23–37, 2017.

[37] Kyle M. Brown, Marna S. Costanzo, Wenxin Xu, Scott Roy, Elena R. Lozovsky, and Daniel L. Hartl. Compensatory mutations restore fitness during the evolution of dihydrofolate reductase. *Mol. Biol. Evol.*, 27(12):2682–2690, 2010.

[38] Gerrit Brandis, Franziska Pietsch, Rahel Alemayehu, and Diarmaid Hughes. Comprehensive phenotypic characterization of rifampicin resistance mutations in salmonella provides insight into the evolution of resistance in mycobacterium tuberculosis. *Journal of Antimicrobial Chemotherapy*, 70(3):680–685, 2015.

[39] HP Lambert. Don't keep taking the tablets? *The Lancet*, 354(9182):943–945, 1999.

[40] Martin J Llewelyn, Jennifer M Fitzpatrick, Elizabeth Darwin, Cliff Gorton, John Paul, Tim EA Peto, Lucy Yardley, Susan Hopkins, Ann Sarah Walker, et al. The antibiotic course has had its day. *Bmj*, 358, 2017.

Supporting Information

Suman G. Das, Muhittin Mungan, Joachim Krug

Supporting Information Text

A Mutation number in fitness maxima

As noted in the main text, there is a typical number of mutations in fitness maxima that depends on the drug concentration. We provide an intuitive argument for understanding this. The log-fitness F is given by

$$F = -\sum_i \sigma_i u_i - \log\left(1 + e^{\alpha\left(\chi - \sum_i \sigma_i v_i\right)}\right). \tag{S1}$$

For large χ, the number of mutations q in a high-fitness genotype is large, and as a crude approximation we can make the replacements $\sum_i \sigma_i u_i \to q\bar{u}$ and $\sum_i \sigma_i v_i \to q\bar{v}$, where $\bar{u}$ and $\bar{v}$ are averages over the full set of L mutations. This gives us the approximation

$$F = -q\bar{u} - \log\left(1 + e^{\alpha(\chi - q\bar{v})}\right). \tag{S2}$$

It is now straightforward to show that the leading order approximation to q at which the above expression is maximized is given by $q^* = \chi/\bar{v}$.

B Sharp transition between phases

The transition from the directed to the fluctuating phase is *sharp* in the sense that it occurs on a time-scale that is much faster than the time-scales of the individual phases. To show this, we focus on the mean fixation probability of the beneficial mutations that can occur on the evolving genotype. This quantity is plotted in Figure S1A for system sizes $L = 100, 200$ as a function of the rescaled time t/L. The curves collapse in the directed and fluctuating phases, but not in the intermediate transition region, where the curve is steeper for larger system size. This indicates that the time-scale associated with the individual phases is $O(L)$, but the transition occurs on faster scale. In Fig S1B, we show that rescaling the time axis by $\sqrt{L}$ (after an appropriate shift of origin by a_L) leads to the steep part of the curves (representing the transition) collapsing on each other. This implies that the time-scale of the transition is $O(\sqrt{L})$, which is much shorter than the time-scale of the walk.

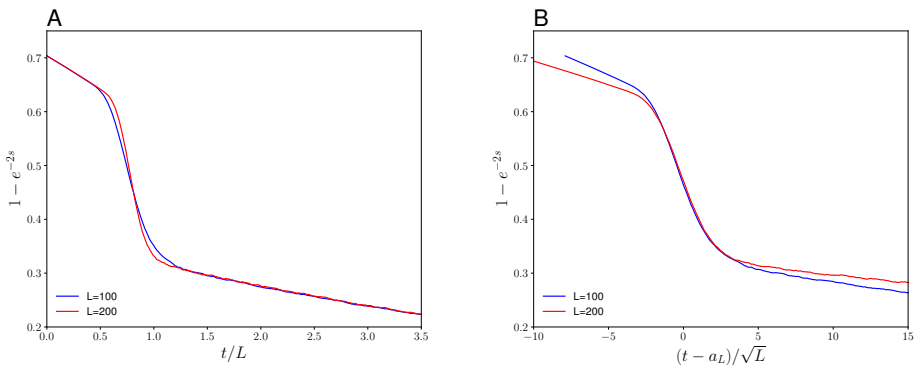

Figure S1: (A) The mean fixation probability of fitter neighbors of the evolving genotype as a function of time is shown for two different system sizes. The concentrations for both sizes are $\chi = \frac{1}{2}\bar{v}L$. On the x-axis, t is the number of time steps, as defined in the main text. The time axis has been rescaled by L for both of the curves. (B) The same data is shown, except that the curves have been shifted along the time-axis by $a_{100} = 79$ and $a_{200} = 158$, respectively, which were chosen to center the curves around zero. The time axis has now been rescaled by $\sqrt{L}$.

C Shape of dose-response curves and existence of the directed phase

We determine the conditions under which adaptive walks starting from the wild type will display an initial phase containing only forward mutations when the concentration is sufficiently high. Consider a dose-response curve (in untransformed variables) of the form

$$f(x) = r_{\boldsymbol{\sigma}} w\left(x/m_{\boldsymbol{\sigma}}\right), \tag{S3}$$

where $w(\cdot)$ is a continuous, monotonic decreasing function that goes to zero as $x \to \infty$. Converting to logarithmic scale, the log-fitness is

$$F(\chi) = -u_{\boldsymbol{\sigma}} + \log w\left(e^{\chi - v_{\boldsymbol{\sigma}}}\right). \tag{S4}$$

We will find *conditions on the shape of* $w(\cdot)$ *which ensure that, given any mutation* (u_i, v_i) *which is beneficial at* some *concentration, the reversal of it must be deleterious if* χ *is sufficiently high.* We show below that a sufficient condition for this to happen is that the DRC's of a genotype and its single-mutation neighbor intersect at most once, *i.e.* the fitness difference of the two mutational neighbors cross the χ-axis at most once.

A forward mutation (u_i, v_i) is beneficial in a background of resistance level v at concentration χ if and only if

$$\log \frac{w\left(e^{\chi - v + v_i}\right)}{w\left(e^{\chi - v}\right)} > u_i. \tag{S5}$$

The inequality is violated at $\chi = -\infty$ (corresponding to $x = 0$). Now, if the DRC's of the background genotype and the mutant can intersect at most once, then the two sides of Eq. (S5) are equal at most at one value of χ (call it $\chi_i^\dagger(v)$). This implies that for any given values of (u_i, v_i) and v, Eq. (S5) can be satisfied if and only

$$\lim_{\chi\to\infty} \log \frac{w\left(e^{\chi+v_i}\right)}{w\left(e^{\chi}\right)} > u_i. \tag{S6}$$

If the condition is not satisfied, the mutation is not beneficial at any concentration in any background; if it is satisfied, then the mutation is beneficial (or equivalently, its reversal is deleterious) at sufficiently high concentration (*i.e.*, when $\chi > \chi_i^\dagger(v)$). This proves the desired result, namely that a sufficient condition for the existence of a directed phase is that the DRC's of mutational neighbors can intersect at most once. It was shown in [1] that this condition is satisfied by most functions $w(\cdot)$ used to model DRC's.

Note that Eq. (S6) holds for the Hill function $w(x) = (1 + x^\alpha)^{-1}$ when $u_i < \alpha v_i$, as shown in the main text. Further, the condition holds without any restriction on the relationship between u_i and v_i when the slope of $-\log W(\chi)$ (where $W(\chi) = w(e^\chi)$) increases without bound as $\chi \to \infty$. This is true when the asymptotic decay of $w(x)$ is faster than a power law (e.g., when $w(x) \sim \exp(-x^a)$ for any $a > 0$).

References

[1] Suman G Das, Susana OL Direito, Bartlomiej Waclaw, Rosalind J Allen, and Joachim Krug. Predictable properties of fitness landscapes induced by adaptational tradeoffs. *Elife*, 9:e55155, 2020.

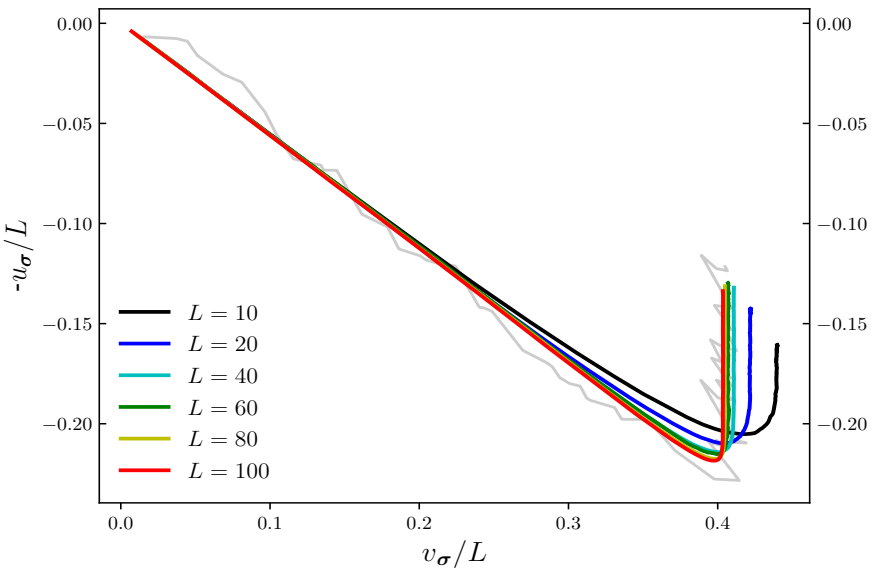

Figure S2: The solid curves show the mean null fitness versus the mean resistance for Kimura adaptive walks for various genome sizes. The grey line shows a single trajectory for $L = 100$. The distribution used in the plots is the given in the Methods section of the main text, with the parameter $\mu = 0$. The axes have been scaled with system size L to facilitate comparison of the relative degree of null-fitness compensation across system sizes. The compensation increases with system size, since for larger sizes, values of u_i closer to zero occur with higher probability in the landscape. The degree of compensation appears to saturate at large system sizes.